

Design, synthesis and biological evaluation of novel indano- and thiaindano-pyrazoles with potential interest for Alzheimer's disease†

Cite this: DOI: 10.1039/c3md00041a

David Genest,^{ab} Christophe Rochais,^{*ab} Cédric Lecoutey,^{ab} Jana Sopkova-de Oliveira Santos,^{ab} Céline Ballandonne,^{ab} Sabrina Butt-Gueulle,^{ab} Remi Legay,^{ab} Marc Since^{ab} and Patrick Dallemagne^{ab}

Received 7th February 2013

Accepted 4th April 2013

DOI: 10.1039/c3md00041a

www.rsc.org/medchemcomm

The synthesis of eighteen novel (thia)indanopyrazole derivatives was achieved starting from amino(thia)indanones. Some of them displayed a dual binding site acetylcholinesterase inhibition which makes them potentially interesting for Alzheimer's disease treatment.

1 Introduction

Since a cholinergic hypothesis has been postulated as a crucial element in Alzheimer's Disease (AD) symptoms etiology, catalytic acetylcholinesterase (AChE) inhibitors have constituted until today the main drugs used against AD.¹ It seems however necessary today to complete this symptomatic approach with a more disease-modifying one, these two activities being able to be associated in a single chemical compound. Such Multi-Target-Directed Ligands (MTDL) have been proposed.^{2–10} Among them, Dual Binding Site (DBS) AChE inhibitors appear as promising anti-AD agents^{11–13} and several novel inhibitors have been developed.^{14–25} In fact, they have the potential to restore the cholinergic deficit by inhibiting the catalytic site (CAS) of AChE and at the same time to reduce the A β deposition and aggregation through their interaction with the peripheral anionic site (PAS)²⁶ of the enzyme. Indeed the PAS is implicated in a stable complex with A β and promotes its aggregation. Donepezil itself, a widely used AD drug, is an AChE DBS inhibitor, inhibits fibrillogenesis (%inhibition = 22% at 100 μ M)¹² and appears more efficient than the other catalytic AChE inhibitors in the latest stages of the disease.²⁷

The distance separating the two AChE sites is about 14 Å and consequently it is possible to design appropriate DBS inhibitors with relatively small compounds conserving a correct pharmacokinetic profile. For this purpose, we recently have

performed a study which led to the design of a DBS AChE inhibition pharmacophore.²⁸ The latter appears particularly useful to design some novel DBS inhibitors starting from CAS AChE inhibitors.

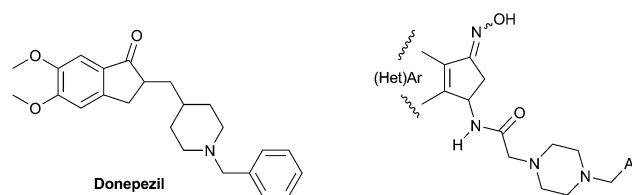


Fig. 1 Structure of donepezil and general structure of (thia)indano pyrazole AChE inhibitors.

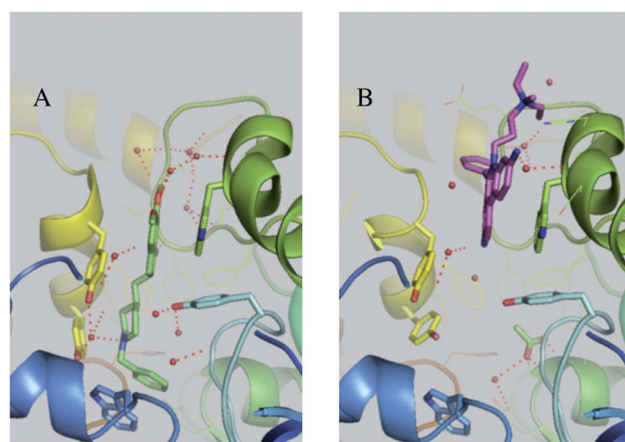


Fig. 2 The AChE binding sites from the X-ray structure of complexes with (A) donepezil (PDB ID: 4EY7) and (B) with propidium (PDB ID: 1N5R). The protein is represented as a ribbon, the side chains of binding site residues are in stick representation and red balls represent water molecules. This figure was made with PYMOL (DeLano Scientific, 2002, San Carlo, USA).

^aNormandie Université, France

^bUniversité de Caen Basse-Normandie, Centre d'Etudes et de Recherche sur le Médicament de Normandie (EA 4258 - FR CNRS 3038 INC3M - SF 4206 ICORE) UFR des Sciences Pharmaceutiques, Bd Becquerel, F-14032 Caen, France. E-mail: christophe.rochais@unicaen.fr; Fax: +33-231-566-803; Tel: +33-231-566-803

† Electronic supplementary information (ESI) available: Full experimental procedures and characterization data for reported compounds including X-ray structures of compounds **2b** and **7a**. CCDC 899872 and 899873. For ESI and crystallographic data in CIF or other electronic format see DOI: 10.1039/c3md00041a

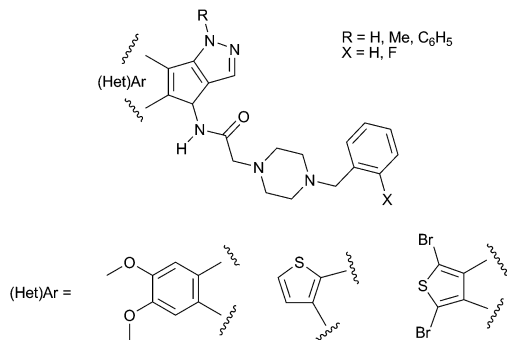


Fig. 3 Targeted structures.

A few years ago, we performed the synthesis of numerous (thia)indano derivatives, among which some analogs of donepezil exhibited potent catalytic electric eel (ee) AChE inhibition (Fig. 1).²⁹

In order to obtain a DBS inhibition profile for this series, we performed a molecular modeling study in which we compared the AChE binding sites from the X-ray structure of complexes with donepezil and propidium, a reference PAS inhibitor which strongly inhibits fibrillogenesis (%inhibition = 82% at 100 μ M) (Fig. 2).¹² This study suggested that the introduction of a third fused ring on the thiaindane moiety of MR 26086 could enhance its interaction with the PAS of AChE. We wish to report herein the results obtained with the synthesis of some indano and thiaindanopyrazole derivatives (Fig. 3).

2 Chemistry

The access to targeted compounds was achieved starting from trifluoroacetylthiaindanones (**1a–c**) that we previously described (Scheme 1).^{30–32} The latter were treated by DMF–DMA in refluxing toluene to give the enamines **2a–c** in quantitative

yields.³³ The *E* geometry of the latter was established by NOE experiments and confirmed by the X-ray structure of **2b**.³⁴ The pyrazole derivatives **3a–c**, **4a–c** and **5a–c** were quantitatively obtained by treating **2a–c** in boiling acetic acid with hydrazine sulfate, methylhydrazine and phenylhydrazine respectively.^{35–38} Acidic hydrolysis yielded the hydrochloric salts of the (thia)indano-pyrazolamines **6** to **8a–c**. Concerning the *N*-substituted derivatives **4a–c**, **5a–c**, **7a–c** and **8a–c** the methyl group and phenyl ring were selectively borne by the *N*-1 atom as observed through NMR experiments and confirmed by X-ray diffractometry of **7a**.³⁴

The amino group of the synthesized tricyclic compounds was then converted into a haloalkyl carboxamide one with chloroacetyl chloride in DCM at 0 °C in the presence of TEA. The sequence led to the carboxamides **9** to **11a–c** in good yields.

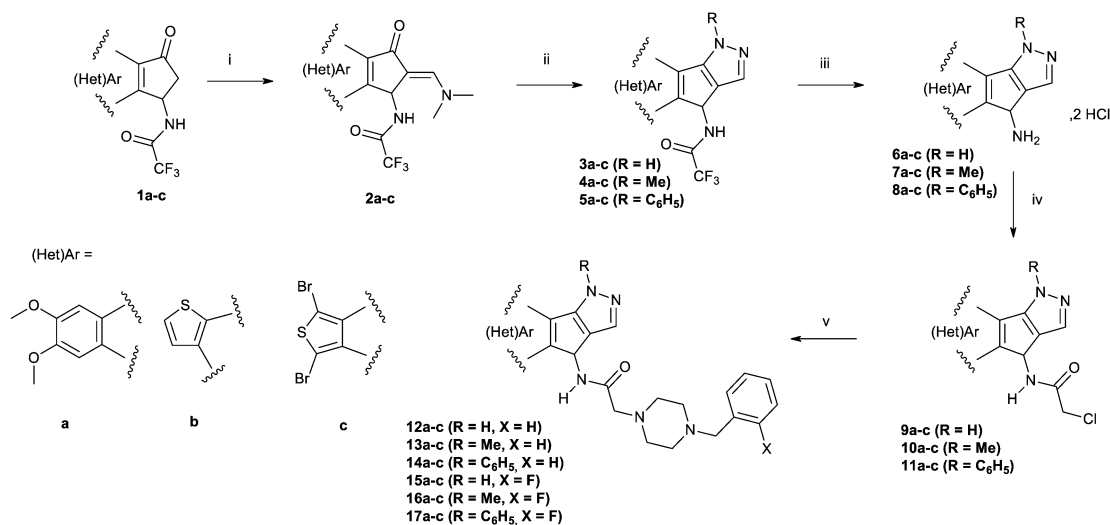
Finally the targeted structures **12** to **17a–c** were obtained by treating **9** to **11a–c** with *N*-benzyl and 2-fluorobenzyl piperazines respectively in the presence of K_2CO_3 in refluxing acetone.

3 Biology

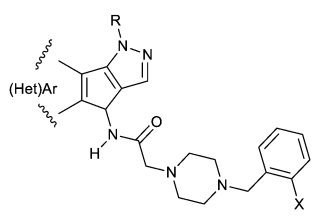
Compounds **12** to **17a–c** were first evaluated as potential inhibitors of electric eel (ee) AChE according to Ellman's test,³⁹ donepezil being used as a control (Table 1). Some of them were further evaluated against human (h) AChE and equine (eq) butyrylcholinesterase (BuChE). Finally, displacement of propidium iodide from the PAS of eeAChE was performed for selected compounds using donepezil as a control.⁴⁰

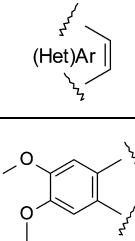
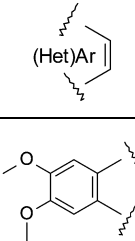
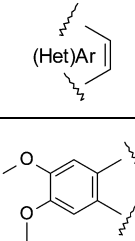
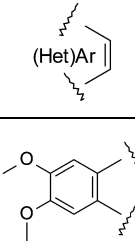
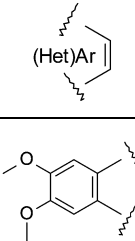
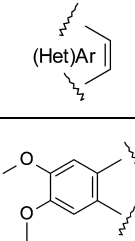
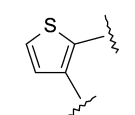
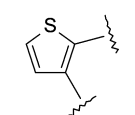
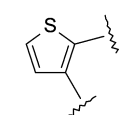
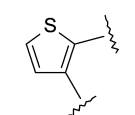
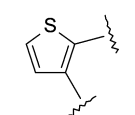
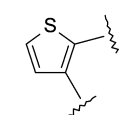
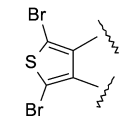
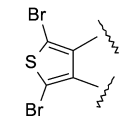
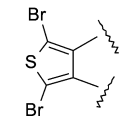
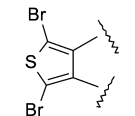
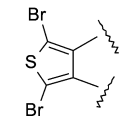
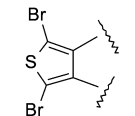
3.1 Results

Concerning the catalytic inhibition of eeAChE, among the eighteen tested compounds, five of them (**13c**, **17a**, **16c**, **14c** and **16a**) exhibited submicromolar IC_{50} , whereas donepezil inhibited the CAS of the enzyme with an IC_{50} of 20 nM. Compounds were further evaluated against hAChE. The inhibitory activities



Scheme 1 Chemical pathway to targeted structures **12** to **17a–c**. Reagents and conditions: (i) DMF–DMA, toluene, reflux, 8 h; (ii) NH_2NH_2 , H_2SO_4 (R = H) or NH_2NHR (R = Me, C_6H_5), AcOH, reflux, 4 h; (iii) 6 M HCl, reflux, 2 h; (iv) $ClCH_2COCl$, TEA, DCM, 0 °C to rt, 1 h; (v) benzylpiperazine, 2HCl (X = H) or 2-fluorobenzylpiperazine (X = F), K_2CO_3 , acetone, oil bath reflux or microwave irradiation.

Table 1 Inhibition of eeAChE, hAChE, and eq BuChE for compounds **12** to **17a–c** and propidium iodide competition assay for selected compounds


Compound	(Het)Ar	X	R	eeAChE IC ₅₀ (μM) or (%) inh 10 ⁻⁵ M	hAChE IC ₅₀ (μM) or (%) inh 10 ⁻⁵ M	Eq BuChE IC ₅₀ (μM) or (%) inh 10 ⁻⁵ M	Propidium iodide displacement (%) inh 10 ⁻⁵ M
12a			H	2.94	49%	NT ^a	NT ^a
13a		H	Me	1.28	1.84	NT	NT
14a			C ₆ H ₅	1.36	2.99	NT	NT
15a		F	H	3.98	50%	NT	NT
16a			Me	0.72	2.44	1%	11% ± 1, n = 3
17a			C ₆ H ₅	0.21	2.43	8%	12% ± 2, n = 4
12b			H	49%	9.18	NT	NT
13b		H	Me	1.91	0.93	NT	NT
14b			C ₆ H ₅	31%	36%	NT	NT
15b		F	H	4.59	42%	NT	NT
16b			Me	1.31	1.32	NT	NT
17b			C ₆ H ₅	4.06	42%	NT	NT
12c			H	8.82	1.13	NT	NT
13c		H	Me	0.10	0.33	7.76	15% ± 1, n = 3
14c			C ₆ H ₅	0.29	0.87	37%	14% ± 3, n = 3
15c		F	H	4.53	42%	NT	NT
16c			Me	0.24	0.88	30%	7% ± 3, n = 3
17c			C ₆ H ₅	27%	15%	NT	NT
Donepezil	—	—	—	0.020	0.011	NT	19% ± 3, n = 2

^a NT: not tested.

of the five selected compounds were globally correlated between the two enzymes with IC₅₀ three times higher against hAChE, except for **17a** whose IC₅₀ differs by a factor twelve between hAChE and eeAChE. This difference could be explained by the fact that the hAChE aromatic gorge is narrower than in other species which could lead to conformational flip of the piperidine ring in donepezil.⁴¹ As described by Cheung *et al.*⁴¹ these differences in the gorge shape could affect generally the binding of long inhibitors such as DBS inhibitors. Furthermore, all of them acted as a selective inhibitor of AChE over BuChE.

The five selected compounds were further tested to evaluate their capacity to displace propidium iodide from the PAS of eeAChE. Two of them (**13c** and **14c**) displaced propidium in a slightly weaker manner (%inhibition of the fluorescence of propidium bound to AChE = 14–15% at 10 μM) than donepezil (19%), whereas **16c** appeared weaker (7%).

Consequently, we studied the mechanism of AChE inhibition for compounds **13c** and **16c** by means of a kinetic study, the results of which are reported in a typical Lineweaver–Burk plot (Fig. 4). For **16c**, the study accounted for a non-competitive inhibition, its inhibition constant (*K_i*) being equal to 429 nM. For **13c**, for which *K_i* was equal to 235 nM, the kinetic profile accounted for a reversible, mixed-type model of inhibition, in accordance with a likely DBS mode of interaction with AChE.⁴²

3.2 SAR discussion

These results show firstly that the benzylpiperazine–carboxamide moiety borne by a (thia)indanopyrazole system is likely to conserve the catalytic AChE inhibition exerted by the (thia)indane series and to display further interactions with the PAS of the enzyme. However, in a similar manner to that of the (thia)indane series,²⁸ the nature and the substitutions of the aromatic ring appear crucial for the catalytic inhibition of the enzyme since the members of the cyclopenta[*b*]thiophene series (**b**) appear less active than those of the dibromocyclopenta[*c*]thiophene (**c**) and dimethoxyindane (**a**) series. The presence of a fluorine atom on the benzyl ring seems likely to maintain or to slightly improve the activity in regard to the corresponding unsubstituted compounds, except for **17c**, which has totally lost the activity expressed by **14c**.

On the other hand, substitution of the N-1 atom of the pyrazole ring by a methyl group appears important for the catalytic inhibition of AChE since *N*-methyl compounds (**13a–c** and **16b,c**) are generally more potent than the unsubstituted or phenyl substituted corresponding compounds. The most potent catalytic inhibitor in this series is **13c** (eeAChE-IC₅₀ = 100 nM, hAChE-IC₅₀ = 330 nM).

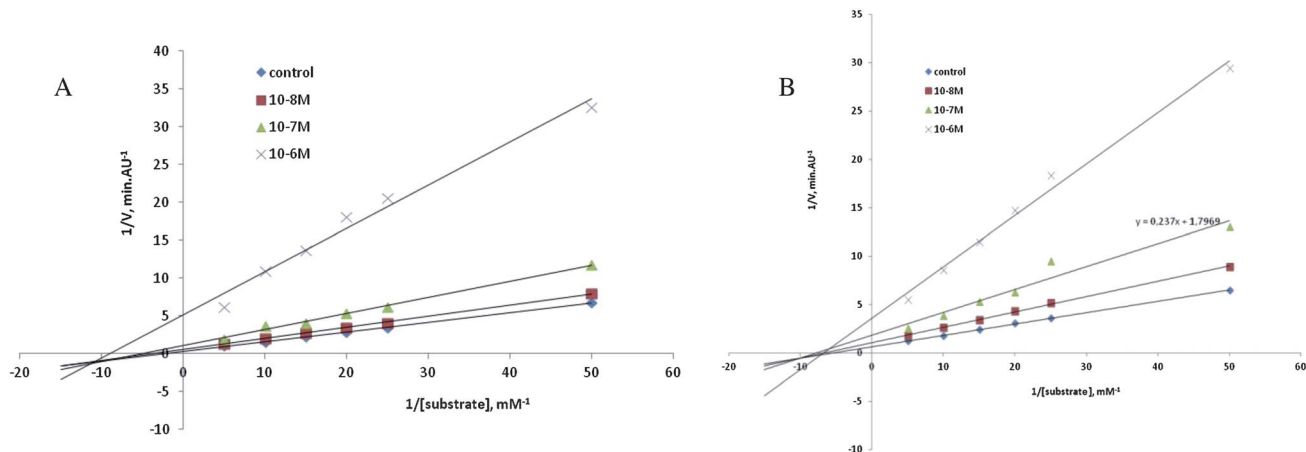


Fig. 4 Lineweaver–Burk plots of inhibition kinetics for **13c** (A) and **16c** (B): reciprocals of enzyme activity (eeAChE) vs. reciprocal of substrate (acetylthiocholine) concentration in the presence of different concentrations of tested compounds.

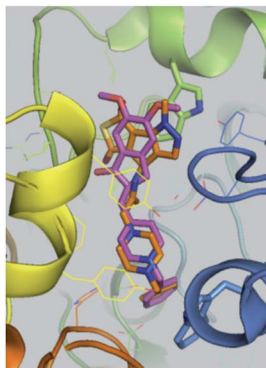


Fig. 5 Compound **13c** (orange) and donepezil (magenta) positioned in the AChE binding site from docking studies. The protein is represented as a ribbon, the side chains of binding site residues are in stick representation. This figure was made with PYMOL (DeLano Scientific, 2002, San Carlo, USA).

Concerning the DBS inhibition, the latter is observed especially in dibromocyclopenta[*c*]thiophene series (compounds **13c** and **14c**) which displace propidium from the PAS of AChE with the same range of activity than donepezil. Compound **16c**, the fluoro analog of **13c**, however does almost not interact with the PAS of the enzyme. These results are supported by the kinetic study of these compounds.

4 Molecular modeling

The docking of **13c**, the best synthesized ligand in our series, showed that its position in the AChE binding site remains very close to the donepezil one, in spite of the presence of the pyrazole ring (Fig. 5). Along the docking pose, **13c** appears to be capable of interacting with the AChE CAS and PAS and it can be considered as a DBS inhibitor. However the introduction of the pyrazole ring led to a different position of the tricycle which did not improve its interaction with the PAS. These observations are correlated with the experimental results showing the same level in the propidium displacement for **13c** and donepezil.

5 Conclusion

In conclusion, during this work we have synthesized several novel (thia)indanopyrazole derivatives and some of them strongly inhibit the catalytic activity of electric eel and human AChE in a submicromolar range of magnitude and further displace propidium from the PAS of the enzyme in a similar manner to that of donepezil. The latter result accounts for a potential inhibitory effect against AChE-induced A β aggregation likely to complete the capacity of these MTDL to preserve cholinergic neuro-transmission in the AD experimental model. This work is under investigation.

6 Experimental part

6.1 General

All commercial solvents and reagents were used as-received.

The microwave reactions were performed using a Biotage Initiator Microwave oven using 2–5 mL sealed vials; temperatures were measured with an IR-sensor and reaction times given as hold times. Flash chromatography was realized on a spot 2 apparatus. Melting points were determined on a Kofler melting point apparatus and were uncorrected. IR spectra were recorded on KBr discs; only selected absorbances were quoted. TLC was carried out on 5 × 10 pre-coated plates with silica gel GF254 type 60; LC/MS (ESI) analyses were realized with a separating module using the following gradient: A (95%)/B (5%) to A (5%)/B (95%) in 5 min; this ratio was held for 2 min before returning to initial conditions in 1 min. Initial conditions were then maintained for 2 min (A: H₂O, B: CH₃CN; each containing HCOOH: 0.1%; column: C18, flow: 0.4 mL min⁻¹). MS detection was performed by positive or negative ESI. High resolution mass spectra were recorded at 40 eV by electronic impact (HREIMS) or positive or negative electrospray (HRESIMS). ¹H and ¹³C NMR spectra were recorded, respectively, at 400 and 100 MHz using CDCl₃, d₆-DMSO, CD₃OD or (CD₃)₂CO as solvents. 2D NMR spectra and 1D NOESY experiments were recorded at 500 MHz. The apparent multiplicity is described as s (singlet), d (doublet),

dd (doublet of doublets), t (triplet), q (quadruplet), m (multiplet); chemical shifts δ are reported in parts per million with the solvent resonance as the internal standard; coupling constants J are given in Hertz.

6.2 Chemistry

6.2.1 *N*-{(2*E*)-2-[(Dimethylamino)methylene]-5,6-dimethoxy-3-oxo-2,3-dihydro-1*H*-inden-1-yl]-2,2,2-trifluoroacetamide (2a). To a suspension of 10 g of **1a** (33 mmol) in toluene (150 mL) was added DMF-DMA (8.8 mL, 2 equiv.). The suspension was then heated at reflux for 8 h, then cooled to room temperature and concentrated under reduced pressure. The resulting orange powder obtained was triturated in ice-cold ether and filtered, which led to **2a** as a yellow powder (11.1 g, 94%); mp > 260 °C; IR (KBr) λ (cm⁻¹) 2999, 2972, 2937, 2839, 1702, 1663, 1589, 1533, 1501, 1472, 1436, 1360, 1310, 1283, 1207, 1184, 1145, 1128, 1097, 1033, 999; ¹H NMR (400 MHz, CDCl₃) δ 8.26 (d, J = 7.83 Hz, 1H, NH), 7.05 (s, 1H, CHNMe₂), 7.04 (s, 1H, H phenyl), 7.01 (s, 1H, H phenyl), 6.25 (1H, d, J = 8.79 Hz, CHNH), 3.92 (3H, s, OCH₃), 3.90 (3H, s, OCH₃), 3.06 (6H, s, NMe₂); ¹³C NMR (100 MHz, CDCl₃) δ 191.0, 157.8 (q, J = 37.4 Hz, COCF₃), 153.9, 150.2, 147.4 (2C), 141.8, 131.3, 116.2 (q, J = 287.8 Hz, COCF₃), 106.4, 103.4, 103.0, 56.4, 56.0, 50.0 (2C); HREIMS [M⁺] m/z 359.1219 (calcd for C₁₆H₁₇F₃N₂O₄ 359.1219).

6.2.2 *N*-(6,7-Dimethoxy-2,4-dihydroindeno[1,2-*c*]pyrazol-4-yl)2,2,2-trifluoroacetamide (3a). To a suspension of 5 g of **2a** (14 mmol) in AcOH (30 mL) was added hydrazine sulfate (2.18 g, 16.7 mmol, 1.2 equiv.). The suspension was then heated at reflux for 4 h, then cooled to room temperature and concentrated under reduced pressure. The crude mixture was then triturated in water, filtered and dried under air. This led to **3a** as a yellow powder (4.34 g, 95%); mp > 260 °C; IR (KBr) λ (cm⁻¹) 3271, 1702, 1550, 1486, 1386, 1284, 1212, 1187, 1156, 1034; ¹H NMR (400 MHz, d₆-DMSO), δ 12.67 (s, 1H, NH pyrazole), 10.00 (d, J = 5.8 Hz, NHCOCF₃), 7.66 (s, 1H, H pyrazole), 7.18 (s, 1H, H phenyl), 7.05 (s, 1H, H phenyl), 5.74 (d, J = 5.8 Hz, 1H, CHNH), 3.83 (s, 3H, OCH₃), 3.76 (s, 3H, OCH₃); ¹³C NMR (100 MHz, d₆-DMSO) δ 157.6, 157.5 (q, J = 35.7 Hz, COCF₃), 149.8, 148.4, 140.7, 127.2, 124.8, 123.5, 116.1 (q, J = 287.4 Hz, COCF₃), 109.7, 103.4, 55.9 (2C), 48.0; HRESIMS [M + H] m/z 328.0984 (calcd for C₁₄H₁₂F₃N₃O₃ 328.0909).

6.2.3 6,7-Dimethoxy-1,4-dihydroindeno[1,2-*c*]pyrazol-4-amine dihydrochloride (6a). Trifluoroacetamide **3a** (2 g, 6.11 mmol) was suspended in 6 M HCl solution (15 mL) and refluxed for 2 h. The solvent was evaporated under reduced pressure and the crude powder was triturated in ice-cold EtOH, filtered, triturated in ice-cold ether and filtered again. This led to **6a** as a yellow powder (1.52 g, 82%); mp 227–229 °C; IR (KBr) λ (cm⁻¹) 2915, 2599, 1624, 1585, 1505, 1461, 1441, 1280, 1221, 1129, 1058, 1027; ¹H NMR (400 MHz, d₆-DMSO) δ 8.90 (d, J = 5.2 Hz, 3H, NH₃⁺Cl⁻), 7.72 (s, 1H, H pyrazole), 7.70 (s, 1H, H phenyl), 7.22 (s, 1H, H phenyl), 5.07 (q, J = 5.2 Hz, 1H, CHNH₃⁺Cl⁻), 3.84 (s, 3H, OCH₃), 3.79 (s, 3H, OCH₃); ¹³C NMR (100 MHz, d₆-DMSO) δ 157.5, 150.0, 148.2, 138.0, 127.2, 126.3, 121.3, 110.9, 103.5, 55.9, 47.3, 34.2; HRESIMS [M + H] m/z 232.1085 (calcd for C₁₂H₁₃N₃O₂ 232.1086).

6.2.4 2-Chloro-*N*-(6,7-dimethoxy-1,4-dihydroindeno[1,2-*c*]pyrazol-4-yl)acetamide (9a). To a suspension of **6a** (500 mg, 1.64 mmol) in DCM (10 mL) was added TEA (0.71 mL, 5.26 mmol, 3.2 equiv.). After 5 min, the mixture was cooled in an ice bath and a solution of chloroacetyl chloride (144 μ L, 1.80 mmol, 1.1 equiv.) in DCM (10 mL) was added drop-wise. When the addition was over, the ice bath was removed and the mixture was stirred for 1 h. The solvent was then evaporated under reduced pressure and the crude powder was triturated in water, filtered and dried under air. This led to **9a** as a white powder (364 mg, 72%); mp 200–202 °C; IR (KBr) λ (cm⁻¹) 2933, 1655, 1592, 1518, 1485, 1465, 1434, 1384, 1281, 1215, 1186, 1173, 1136, 1034; ¹H NMR (400 MHz, CDCl₃) δ 7.50 (s, 1H, H pyrazole), 7.29 (s, 1H, H phenyl), 7.08 (s, 1H, H phenyl), 6.78 (d, J = 7.79 Hz, 1H, NH acetamide), 5.92 (d, J = 7.79 Hz, 1H, CHNH), 4.19 (d, J = 15.6 Hz, 1H, Ha), 4.14 (d, J = 15.6 Hz, 1H, Hb), 3.96 (s, 3H, OCH₃), 3.93 (s, 3H, OCH₃); ¹³C NMR (100 MHz, CDCl₃) δ 166.7, 159.2, 150.3, 149.5, 141.4, 126.9, 124.8, 124.5, 109.2, 103.8, 56.4, 56.3, 48.6, 42.6; HREIMS [M⁺] m/z 307.0709 (calcd for C₁₄H₁₄ClN₃O₃ 307.07234).

6.2.5 2-(4-Benzylpiperazin-1-yl)-*N*-(6,7-dimethoxy-1,4-dihydroindeno[1,2-*c*]pyrazol-4-yl)acetamide (12a). Chloroacetamide **9a** (100 mg, 0.32 mmol), benzylpiperazine dihydrochloride (89 mg, 0.36 mmol, 1.1 equiv.) and K₂CO₃ (144 mg, 1.04 mmol, 3.2 equiv.) were refluxed in acetone (2 mL) for 12 h. After being cooled to ambient temperature, the crude mixture was filtered and the insoluble product was washed with DCM. The filtrates were combined and the solvents were evaporated under reduced pressure. The crude powder obtained was then purified by column chromatography (Al₂O₃, gradient from MeOH/DCM 0/100 to 10/90). This led to **12a** as a yellow powder (51 mg, 35%); mp 152 °C; IR (KBr) λ (cm⁻¹) 2929, 2834, 1662, 1581, 1492, 1445, 1380, 1288, 1223, 1134, 1031; ¹H NMR (400 MHz, CDCl₃) δ 7.45 (s, 1H, H pyrazole), 7.27 (m, 6H, H phenyl), 7.04 (s, 1H, H phenyl), 5.96 (d, J = 7.79 Hz, 1H, CHNH), 3.94 (s, 3H, OCH₃), 3.88 (s, 3H, OCH₃), 3.44 (s, 2H, CH₂ phenyl), 3.15 (d, J = 16.6 Hz, 1H, Ha), 3.10 (d, J = 16.6 Hz, 1H, Hb), 2.54 (broad m, 4H, H piperazine), 2.38 (broad m, 4H, H piperazine); ¹³C NMR (100 MHz, CDCl₃) δ 171.1, 159.1, 149.9, 149.2, 142.4, 137.8, 129.1 (2C), 128.3 (2C), 127.2, 126.7, 125.5, 124.2, 108.8, 103.6, 62.8, 61.6, 56.3, 56.2, 53.5 (2C), 52.9 (2C), 47.7; HRESIMS [M + H] m/z 448.2339 (calcd for C₂₅H₂₉N₅O₃ 448.2349).

6.3 Biology

6.3.1 *In vitro* tests of AChE and BuChE biological activity. Inhibitory capacity of compounds on AChE biological activity was evaluated through the use of the spectrometric method of Ellman. Acetyl- or butyrylthiocholine iodide and 5,5-dithiobis-(2-nitrobenzoic) acid (DTNB) were purchased from Sigma Aldrich. Lyophilized electric eel AChE (Type III, Sigma Aldrich) or BuChE from equine serum (Sigma Aldrich) was dissolved in 0.2 M phosphate buffer pH 7.4 to obtain enzyme stock solutions with 2.5 units per mL enzyme activity. AChE from human erythrocytes (buffered aqueous solution, \geq 500 units per mg protein (BCA), Sigma Aldrich) was diluted in 20 mM HEPES buffer pH 8, 0.1% Triton X-100 to obtain enzyme stock solution

with 2.5 units per mL enzyme activity. In this procedure, 100 μL of 0.3 mM DTNB dissolved in phosphate buffer pH 7.4 were added into the 96 well plate followed by 50 μL of test compound solution and 50 μL of enzyme solution. After 5 min of preincubation, the reaction was then initiated by the injection of 50 μL of 10 mM acetyl- or butyrylthiocholine iodide solution. The hydrolysis of acetyl- or butyrylthiocholine was monitored by the formation of a yellow 5-thio-2-nitrobenzoate anion as the result of the reaction of DTNB with thiocholine, released by the enzymatic hydrolysis of acetyl- or butyrylthiocholine, at a wavelength of 412 nm every minute for 10 min using a 96-well microplate plate reader (TECAN Infinite M200, Lyon, France). Test compounds were dissolved in analytical grade DMSO. Donepezil was used as a reference standard.

First screening of AChE and BuChE activity was carried out at a 10^{-5} M concentration of compounds under study. For the compounds with significant inhibition ($\geq 50\%$) after 4 min of reaction, IC_{50} values were determined graphically from 6 point inhibition curves using the Origin software.

6.3.2 Propidium competition assay. Propidium exhibits an increase in fluorescence on binding to the AChE peripheral site, making it a useful probe for competitive ligand binding to the enzyme. Fluorescence was measured in a Tecan Infinite M200 plate reader. Measurements were carried out in 200 μL solution volume, in 96-well plates. The buffer used was 1 mM Tris-HCl, pH 8.0, 5 U eeAChE which was incubated, for 15 min at 25 $^{\circ}\text{C}$, with a 150 μL 10^{-5} M solution of the compounds or donepezil (from Tocris) as a control. 50 μL of one micromolar propidium iodide solution was added 10 min before the fluorescence measurement. The excitation wavelength was 535 nm, and that of emission was 595 nm. Each assay was repeated, at least, three different times.

6.3.3 *In vitro* tests of AChE kinetic studies. Kinetic studies of compounds on AChE biological activity were performed through the use of the spectrometric method of Ellman. Acetylthiocholine iodide, lyophilized electric eel acetylcholinesterase (Type III, AChE electric eel) and 5,5-dithiobis-(2-nitrobenzoic) acid (DTNB) were purchased from Sigma Aldrich. AChE was dissolved in 0.2 M phosphate buffer pH 7.4 to obtain enzyme stock solutions with 0.25 units per mL AChE activity. In the procedure, 100 μL of 0.3 mM DTNB dissolved in phosphate buffer pH 7.4 were added into the 96 well plate followed by 50 μL of test compound solution and 50 μL of enzyme solution. After 5 min of preincubation, the reaction was then initiated by the addition of 50 μL of different concentrations of acetylthiocholine iodide solution (from 0.02 to 0.2 mM). The hydrolysis of acetylthiocholine was monitored by the formation of yellow 5-thio-2-nitrobenzoate anion as the result of the reaction of DTNB with thiocholine, released by the enzymatic hydrolysis of acetylthiocholine, at a wavelength of 412 nm every minute for 10 min using a 96-well microplate plate reader (TECAN Infinite M200, Lyon, France). Test compounds were dissolved in analytical grade DMSO.

The kinetic studies were performed using four concentrations of the inhibitor (0–1 μM).

6.4 Molecular modeling

The docking of the compound **13c** into human AChE (PDB ID: 4EY7)⁴¹ was carried out with the GOLD program (v5.0) using the default parameters.^{43,44} This program applies a genetic algorithm to explore conformational spaces and ligand binding modes. To evaluate the proposed ligand poses the ChemScore fitness function was applied in the docking studies.

The binding site in the AChE was defined as a 12 \AA sphere centred at the donepezil ligand present in the 4EY7 crystal structure. Furthermore, we paid special attention during the docking procedure to water molecules in the binding site and water HOH931 was included in the binding site during docking.

Acknowledgements

This work was supported through funding from the Ministère Français de l'Enseignement Supérieur et de la Recherche and the Conseil Régional de Basse Normandie (Dispositif de Soutien aux Projets de Recherche Emergents).

Notes and references

- 1 R. T. Bartus, R. L. Dean III, B. Beer and A. S. Lipka, *Science*, 1982, **217**, 408–414.
- 2 M. L. Bolognesi, A. Minarini, V. Tumiatti and C. Melchiorre, *Expert Opin. Ther. Pat.*, 2006, **16**, 811–823.
- 3 M. L. Bolognesi, A. Cavalli, L. Valgimigli, M. Bartolini, M. Rosini, V. Andrisano, M. Recanatini and C. Melchiorre, *J. Med. Chem.*, 2007, **50**, 6446–6449.
- 4 A. Cavalli, M. L. Bolognesi, A. Minarini, M. Rosini, V. Tumiatti, M. Recanatini and C. Melchiorre, *J. Med. Chem.*, 2008, **51**, 347–372.
- 5 J. Sterling, Y. Herzig, T. Goren, N. Finkelstein, D. Lerner, W. Goldenberg, I. Miskolczi, S. Molnar, F. Rantal, T. Tamas, G. Toth, A. Zagyva, A. Zekany, J. Finberg, G. Lavian, A. Gross, R. Friedman, M. Razin, W. Huang, B. Kraiss, M. Chorev, M. B. Youdim and M. Weinstock, *J. Med. Chem.*, 2002, **45**, 5260–5279.
- 6 B. Schmitt, T. Bernhardt, H. J. Moeller, I. Heuser and L. Frolich, *CNS Drugs*, 2004, **18**, 827–844.
- 7 P. Munoz-Ruiz, L. Rubio, E. Garcia-Palomero, I. Dorronsoro, M. del Monte-Millan, R. Valenzuela, P. Usan, C. de Austria, M. Bartolini, V. Andrisano, A. Bidon-Chanal, M. Orozco, F. J. Luque, M. Medina and A. Martinez, *J. Med. Chem.*, 2005, **48**, 7223–7233.
- 8 J. Marco-Contelles, R. Leon, C. de Los Rios, A. Guglietta, J. Terencio, M. G. Lopez, A. G. Garcia and M. Villarroya, *J. Med. Chem.*, 2006, **49**, 7607–7610.
- 9 L. Holmquist, G. Stuchbury, K. Berbaum, S. Muscat, S. Young, K. Hager, J. Engel and G. Munch, *Pharmacol. Ther.*, 2007, **113**, 154–164.
- 10 C. Brühlmann, F. Ooms, P. A. Carrupt, B. Testa, M. Catto, F. Leonetti, C. Altomare and A. Carotti, *J. Med. Chem.*, 2001, **44**, 3195–3198.
- 11 M. Del Monte-Millan, E. Garcia-Palomero, R. Valenzuela, P. Usan, C. de Austria, P. Munoz-Ruiz, L. Rubio,

- I. Dorronsoro, A. Martinez and M. Medina, *J. Mol. Neurosci.*, 2006, **30**, 85–87.
- 12 M. Bartolini, C. Bertucci, V. Cavrini and V. Andrisano, *Biochem. Pharmacol.*, 2003, **65**, 407–416.
- 13 I. Silman and J. L. Sussman, *Curr. Opin. Pharmacol.*, 2005, **5**, 293–302.
- 14 A. Cavalli, M. Bolognesi, S. Capsoni, V. Andrisano, M. Bartolini, E. Margotti, A. Cattaneo, M. Recanatini and C. Melchiorre, *Angew. Chem., Int. Ed.*, 2007, **46**, 3689–3692.
- 15 S. Gupta, A. Fallarero, P. Järvinen, D. Karlsson, M. S. Johnson, P. M. Vuorela and C. G. Mohan, *Bioorg. Med. Chem. Lett.*, 2011, **21**, 1105–1112.
- 16 M. L. Bolognesi, R. Banzi, M. Bartolini, A. Cavalli, A. Tarozzi, V. Andrisano, A. Minarini, M. Rosini, V. Tumiatti, C. Bergamini, R. Fato, G. Lenaz, P. Hrelia, A. Cattaneo, M. Recanatini and C. Melchiorre, *J. Med. Chem.*, 2007, **50**, 4882–4897.
- 17 E. Garcia-Palomero, P. Munoz, P. Usan, P. Garcia, E. Delgado, C. de Austria, R. Valenzuela, L. Rubio, M. Medina and A. Martinez, *Neurodegener. Dis.*, 2008, **5**, 153–156.
- 18 M. I. Fernandez-Bachiller, C. Perez, G. C. Gonzalez-Munoz, S. Conde, M. G. Lopez, M. Villarroja, A. G. Garcia and M. I. Rodriguez-Franco, *J. Med. Chem.*, 2010, **53**, 4927–4937.
- 19 F. Leonetti, M. Catto, O. Nicolotti, L. Pisani, A. Cappa, A. Stefanachi and A. Carotti, *Bioorg. Med. Chem.*, 2008, **16**, 7450–7456.
- 20 L. Pisani, M. Catto, I. Giangreco, F. Leonetti, O. Nicolotti, A. Stefanachi, S. Cellamare and A. Carotti, *ChemMedChem*, 2010, **5**, 1616–1630.
- 21 B. Tasso, M. Catto, O. Nicolotti, F. Novelli, M. Tonelli, I. Giangreco, L. Pisani, A. Sparatore, V. Boido, A. Carotti and F. Sparatore, *Eur. J. Med. Chem.*, 2011, **46**, 2170–2184.
- 22 A. Conejo-Garcia, L. Pisani, C. Nunez Mdel, M. Catto, O. Nicolotti, F. Leonetti, J. M. Campos, M. A. Gallo, A. Espinosa and A. Carotti, *J. Med. Chem.*, 2011, **54**, 2627–2645.
- 23 W. M. Li, K. K. Kan, P. R. Carlier, Y. P. Pang and Y. F. Han, *Curr. Alzheimer Res.*, 2007, **4**, 386–396.
- 24 M. L. Bolognesi, M. Bartolini, A. Tarozzi, F. Morroni, F. Lizzi, A. Milelli, A. Minarini, M. Rosini, P. Helia, V. Andrisano and C. Melchiorre, *Bioorg. Med. Chem. Lett.*, 2011, **21**, 2655–2658.
- 25 M. L. Bolognesi, V. Andrizano, M. Bartolini, R. Banzi and C. Melchiorre, *J. Med. Chem.*, 2005, **48**, 24–27.
- 26 N. C. Inestrosa, A. Alvarez, C. A. Pérez, R. D. Moreno, M. Vicente, C. Linker, O. I. Casanueva, C. Soto and J. Garrido, *Neuron*, 1996, **16**, 881–891.
- 27 R. Howard, R. McShane, J. Lindesay, C. Ritchie, A. Baldwin, R. Barber, A. Burns, T. Denning, D. Findlay, C. Holmes, A. Hughes, R. Jacoby, R. Jones, R. Jones, I. McKeith, A. Macharouthu, J. O'Brien, P. Passmore, B. Sheehan, E. Juszczak, C. Katona, R. Hills, M. Knapp, C. Ballard, R. Brown, S. Banerjee, C. Onions, M. Griffin, J. Adams, R. Gray, T. Johnson, P. Bentham and P. Phillips, *N. Engl. J. Med.*, 2012, **366**, 893–903.
- 28 J. Sopkova-de Oliveira Santos, A. Lesnard, J. H. Agondanou, N. Dupont, A. M. Godard, S. Stiebing, C. Rochais, F. Fabis, P. Dallemagne, R. Bureau and S. Rault, *J. Chem. Inf. Model.*, 2010, **50**, 422–428.
- 29 Z. Omran, T. Cailly, E. Lescot, J. Sopkova-de Oliveira Santos, J. H. Agondanou, V. Lisowski, F. Fabis, A. M. Godard, S. Stiebing, G. Le Flem, M. Boulouard, F. Dauphin, P. Dallemagne and S. Rault, *Eur. J. Med. Chem.*, 2005, **40**, 1222–1245.
- 30 P. Dallemagne, S. Rault, J. C. Pilo, M. P. Foloppe and M. Robba, *Tetrahedron Lett.*, 1991, **44**, 6327–6328.
- 31 P. Dallemagne, S. Rault, M. Cugnon de Sevracourt, K. M. Hassan and M. Robba, *Tetrahedron Lett.*, 1986, **27**, 2607–2610.
- 32 P. Dallemagne, A. Alsaidi, M. Boulouard, S. Rault and M. Robba, *Heterocycles*, 1993, **36**, 287–294.
- 33 H. Bredereck, G. Simchen, S. Rebsdats, K. Willi, P. Horn, R. Wahl, H. Hoffmann and G. Peter, *Chem. Ber.*, 1968, **101**, 41–50.
- 34 Crystallographic data for compounds **2b** CCDC 899873 and **7a** CCDC 899872 have been deposited at the Cambridge Crystallographic Data Centre.
- 35 A.-Z. A. Elasara and A. A. El-Khair, *Tetrahedron*, 2003, **59**, 8463–8480.
- 36 I. Beria, D. Ballinari, J. A. Bertrand, D. Borghi, R. T. Bossi, M. G. Brasca, P. Cappella, M. Caruso, W. Ceccarelli, A. Ciavolella, C. Cristiani, V. Croci, A. De Ponti, G. Fachin, R. D. Ferguson, J. Lansen, J. K. Moll, E. Pesenti, H. Posteri, R. Perego, M. Rocchetti, P. Storici, D. Volpi and B. Valsasina, *J. Med. Chem.*, 2010, **53**, 3532–3551.
- 37 F. Büttner, S. Bergemann, D. Guénard, R. Gust, G. Seitz and S. Thoret, *Bioorg. Med. Chem.*, 2005, **13**, 3497–3511.
- 38 S. Bergemann, R. Brecht, F. Büttner, D. Guénard, R. Gust, G. Seitz, M. T. Stubbs and S. Thoret, *Bioorg. Med. Chem.*, 2003, **11**, 1269–1281.
- 39 G. L. Ellman, K. D. Courtney, V. Andres and R. M. Featherstone, *Biochem. Pharmacol.*, 1961, **7**, 88–95.
- 40 T. L. Rosenberry, W. D. Mallender, P. J. Thomas and T. Szegetes, *Chem.-Biol. Interact.*, 1999, **119–120**, 85–97.
- 41 J. Cheung, M. J. Rudolph, F. Burshteyn, M. S. Cassidy, E. N. Gary, J. Love, M. C. Franklin and J. J. Height, *J. Med. Chem.*, 2012, **55**, 10282–10286.
- 42 M. Catto, L. Pisani, F. Leonetti, O. Nicolotti, A. Stefanachi, S. Cellamare and A. Carotti, *Bioorg. Med. Chem.*, 2013, **21**, 146–152.
- 43 G. Jones, P. Willett and R. C. Glen, *J. Mol. Biol.*, 1995, **245**, 43–53.
- 44 G. Jones, P. Willett, R. C. Glen, A. R. Leach and R. Taylor, *J. Mol. Biol.*, 1997, **267**, 727–748.